A neutron diffraction and NMR study of the *P–T* phase diagram of $Rb_{1-x}(NH_4)_xI$ mixed crystals (x = 0.29,0.77)

2004 J. Phys.: Condens. Matter 16 3889

(http://iopscience.iop.org/0953-8984/16/23/009)

INSTITUTE OF PHYSICS PUBLISHING JOURNAL OF PHYSICS: CONDENSED MATTER

J. Phys.: Condens. Matter **16** (2004) 3889–3900 PII: S0953-8984(04)75776-8

A neutron diffraction and NMR study of the P–T phase diagram of $Rb_{1-x}(NH_4)_xI$ mixed crystals ($x = 0.29, 0.77$)

J Wąsicki[1], S Lewicki[1], D P Kozlenko[2], A Kozak[1], W Nawrocik[1], S E Kichanov[2], B N Savenko[2] and T Shchedrina[2]

[1] Faculty of Physics, A Mickiewicz University, Umultowska 85, 61-614 Poznań, Poland
[2] Frank Laboratory of Neutron Physics JINR, 141980 Dubna Moscow Region, Russia

E-mail: ekich@nf.jinr.ru

Received 30 January 2004
Published 28 May 2004
Online at stacks.iop.org/JPhysCM/16/3889
DOI: 10.1088/0953-8984/16/23/009

Abstract

The structure of $Rb_{1-x}(NH_4)_xI$ ($x = 0.29, 0.77$) mixed crystals was studied by means of powder neutron diffraction in the temperature range 20–300 K and at ambient pressure. Measurements of spin–lattice relaxation time T_1 have been performed for polycrystalline samples of $Rb_{1-x}(NH_4)_xI$ ($x = 0.29, 0.77$) in the temperature range 95–300 K and pressure range 0–800 MPa by the proton NMR technique using the saturation method. Activation parameters were obtained for a model of complex ammonium ion reorientations around two-fold C_2 and three-fold C_3 axes. The activation volume for different phases of the investigated compounds was determined. The experimental data were used for a construction of P–T phase diagram of $Rb_{1-x}(NH_4)_xI$ ($x = 0.29, 0.77$) mixed crystals. The phase diagram of $Rb_{0.23}(NH_4)_{0.77}I$ has similar features to that of NH_4I. Four different phases were found to exist in the temperature and pressure range studied: a disordered α phase with an NaCl-type cubic structure, a disordered β phase with a CsCl-type cubic structure, a γ phase with a tetragonal structure and antiparallel ordering of ammonium ions, and a δ phase with a CsCl-type cubic structure and parallel order of ammonium ions. The phase diagram of $Rb_{0.71}(NH_4)_{0.29}I$ contains only α and β phases, and is similar to that of RbI.

1. Introduction

The ammonium halides are well known for a number of phase transitions they undergo with respect to the disorder and relative orientation of ammonium ions in the lattice [1]. At ambient pressure and room temperature, ammonium iodide NH_4I has an NaCl-type cubic structure

(α phase), space group $Fm\bar{3}m$, in which NH_4^+ ions are located in octahedral coordination of surrounding I^- ions and perform fast reorientational motions between eight equivalent positions in the structure [2]. Recently it was shown that NH_4^+ ions possess an electric dipole moment in this phase [3]. At $T = 256$ K it transforms to a CsCl-type cubic structure (β phase), space group $Pm\bar{3}m$, in which ammonium ions reorient between two energetically equivalent positions [1]. Below $T = 232$ K NH_4I has a tetragonal structure, with an antiparallel ordering of ammonium ions (γ phase), space group $P4/nmm$ [1]. In addition, at moderate pressures $P > 450$ MPa and low temperatures ammonium iodide exhibits a CsCl-type cubic structure with a parallel order of ammonium ions (δ phase), space group $P\bar{4}3m$.

NH_4I is completely miscible with alkali iodides KI and RbI [4]. Solid solutions $(K)_{1-x}(NH_4)_xI$ have the α phase at ambient temperature for all the composition range. Below the critical concentration $x_c \sim 0.55$ $(K)_{1-x}(NH_4)_xI$ compounds exhibit in the low temperature region an orientation glass state driven by frustrated dipolar interactions [3, 5]. In addition, a new ε phase with a trigonal structure (space group $R\bar{3}m$) was detected in these compounds in a narrow concentration range $0.55 < x < 0.75$ [6, 7]. This phase shows a long-range order of the NH_4^+-tetrahedra with two inequivalent ammonium sites. For $0.75 < x < 0.95$ $(K)_{1-x}(NH_4)_xI$ crystals exhibit the β phase and for $x > 0.95$ γ phase was observed. The nature of the orientational glass transition and phase diagram of $(K)_{1-x}(NH_4)_xI$ compounds have been extensively studied by dielectric [3, 8], NMR [9–12] and Raman [13, 14] spectroscopy methods and neutron scattering techniques [6, 7, 15, 16]. In the neutron diffraction studies [15, 16] it was shown that the application of rather moderate pressure $P \sim 500$ MPa leads to a phase transition from α to β phase in $(K)_{1-x}(NH_4)_xI$ systems with $0.35 < x < 0.7$. This means that under high pressure a destabilization of orientational glass state occurs, found to exist in the α phase only.

The $(Rb)_{1-x}(NH_4)_xI$ compounds have been much less studied in comparison with $(K)_{1-x}(NH_4)_xI$ ones. Recent neutron scattering studies of $(Rb)_{1-x}(NH_4)_xI$ reveal the existence of an orientational glass state in the α phase for the composition range $0.29 < x < 0.40$ [17]. For $x > 0.66$, $(Rb)_{1-x}(NH_4)_xI$ compounds were found to exhibit the β phase.

In the present paper, the P–T phase diagram of $Rb_{1-x}(NH_4)_xI$ mixed crystals with ammonium concentrations $x = 0.29$ and 0.77 has been studied by a neutron diffraction method in the temperature range 20–300 K and by NMR spectroscopy at pressures up to 800 MPa.

2. Experiment

Powder samples of $Rb_{1-x}(NH_4)_xI$ mixed crystals with different ammonium concentrations were prepared by slow evaporation of liquid solutions having the corresponding stoichiometric content. Neutron diffraction measurements at ambient pressure and low temperatures down to 20 K were performed with the DN-12 spectrometer [18] at the IBR-2 high flux pulsed reactor, Dubna, Russia. The sample volume was 100 mm^3. The scattering angle was $2\theta = 90°$. The spectrometer resolution was $\Delta d/d = 0.02$ at $d = 2$ Å. A special cryostat constructed on the basis of a closed cycle helium refrigerator was used to create a low temperature on the sample.

Measurements of the spin–lattice relaxation time T_1 were performed on a pulse spectrometer working at frequencies of 59 and 25 MHz by the saturation method. The latter spectrometer was equipped with a special set-up for measurements at hydrostatic pressure [19]. The pressure was generated by a gas compressor U-11 (made by Unipress Warsaw) able to produce pressure up to 1500 MPa, and the measurements were carried out in a pressure cell (made of beryllium bronze) enabling measurements under pressure up to 800 MPa. The measurements were performed over a pressure range from 0.1 to 800 MPa and over a temperature range of 95–300 K. The sample volume was about 1 cm^3.

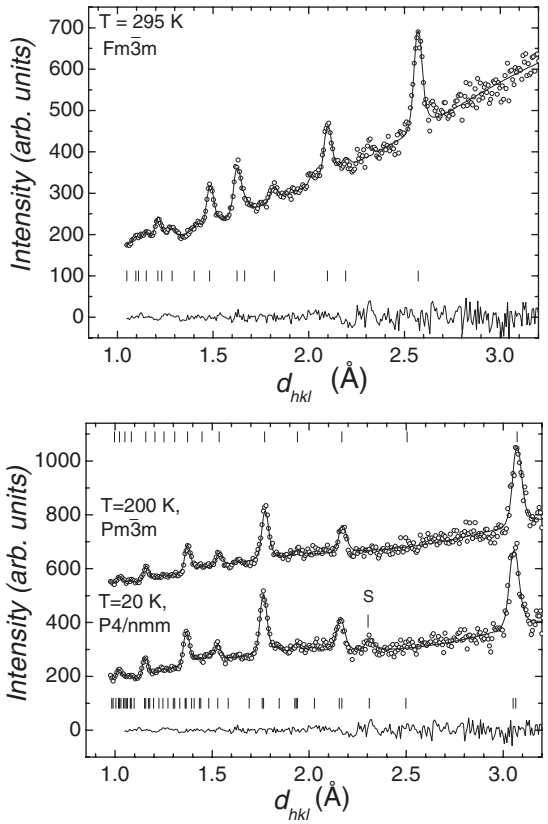

Figure 1. Neutron diffraction patterns of $Rb_{0.23}(NH_4)_{0.77}I$ measured at 295 K (α phase), 200 K (β phase) and 20 K (γ phase) and ambient pressure with the DN-12 spectrometer and processed by the Rietveld method. The experimental points, calculated profiles and difference curves (for $T = 295$ and 20 K) are shown. The tick rows indicate the calculated diffraction peak positions for different phases. The superstructure peak characteristic to the γ phase is marked by the symbol S.

3. Results and discussion

3.1. Neutron diffraction

Neutron diffraction patterns of $Rb_{0.23}(NH_4)_{0.77}I$ measured at $T = 295, 200$ and 20 K are shown in figure 1. At $T = 295$ K the α phase was evidenced in both $Rb_{0.23}(NH_4)_{0.77}I$ and $Rb_{0.71}(NH_4)_{0.29}I$ in agreement with [17], and $Rb_{0.71}(NH_4)_{0.29}I$ remains in this phase down to the lowest temperature of the present study, $T = 20$ K. At $T \sim 200$ K sharp changes characteristic to the α–β phase transition were observed in the diffraction patterns of $Rb_{0.23}(NH_4)_{0.77}I$. Upon further cooling, at $T \sim 150$ K an appearance of the additional superstructure peak at $d_{hkl} = 2.32$ Å was indicated. This peak corresponds to the (211) reflection of the tetragonal γ phase. The γ phase can be considered as a slightly distorted superstructure with respect to the primitive cubic β phase, and the lattice parameters of these phases relate as $a_\gamma \approx a_\beta\sqrt{2}$ and $c_\gamma \approx a_\beta$. The structural parameters of the α phase of $Rb_{0.71}(NH_4)_{0.29}I$ and the α, β and γ phases of $Rb_{0.23}(NH_4)_{0.77}I$ at different temperatures obtained from the Rietveld refinement of the diffraction data using the MRIA program [20] are shown in table 1. The difference between observed and calculated diffraction peak intensities was typically less than 5%.

Table 1. Structural parameters for the α, β and γ phases of $Rb_{1-x}(NH_4)_xI$ crystals ($x = 0.77$, 0.29) at different temperatures and ambient pressure. In the α phase (space group $Fm\bar{3}m$), N/Rb atoms occupy sites 4(b) (0.5, 0.5, 0.5); I atoms sites 4(a) (0, 0, 0); H1 atoms sites 32(f) (x, x, x); and H2 atoms sites 96(k) (x, x, z). In the β phase (space group $Pm\bar{3}m$), N/Rb atoms occupy site 1(b) (0.5, 0.5, 0.5); I atoms site 1(a) (0, 0, 0); and H atoms sites 8(g) (x, x, x). In the γ phase (space group $P4/nmm$), N/Rb atoms occupy sites 2(a) (0, 0, 0); I atoms sites 2(c) (0, 0.5, x_I); and H atoms sites 8(i) (0, x, z).

$Rb_{0.23}(NH_4)_{0.77}I$			
T (K)	295	200	20
phase	α phase ($Fm\bar{3}m$)	β phase ($Pm\bar{3}m$)	γ phase ($P4/nmm$)
Lattice parameters (Å)	$a = 7.272(7)$	$a = 4.343(4)$	$a = 6.125(5)$ $c = 4.304(4)$
Atomic coordinates	—	$x = 0.369(5)$	$x \approx z = 0.132(5)$ $x_I = 0.474(3)$
R_p (%)	1.64	2.05	2.08
R_{wp} (%)	1.47	1.76	1.82
$Rb_{0.71}(NH_4)_{0.29}I$			
T (K)	295	200	20
phase		α phase ($Fm\bar{3}m$)	
Lattice parameter (Å)	$a = 7.306(7)$	$a = 7.291(7)$	$a = 7.254(5)$
R_p (%)	2.12	2.12	2.18
R_{wp} (%)	1.82	1.84	1.98

Due to the presence of strong incoherent background from hydrogen atoms in the diffraction patterns, it was impossible to obtain the coordinates of hydrogens for the α-phase. In this phase NH_4^+ ions are disordered between eight equivalent positions with one H atom located at sites 32(f) (x, x, x) and three H atoms at sites 96(k) (x, x, z) of the space group $Fm\bar{3}m$. The N–H bond length calculated from the obtained hydrogen coordinates (see table 1) for the β and γ phases of $Rb_{0.23}(NH_4)_{0.77}I$, $l_{N-H} = 0.99(3)$ Å, agrees within experimental accuracy with the value $l_{N-H} = 1.03$ Å, obtained in previous investigations of ammonium halides [21]. At ambient temperature the lattice parameter of the α-phase of $Rb_{1-x}(NH_4)_xI$ decreases linearly as a function of NH_4I concentration x, $a(x) = 7.34 - 0.082x$, in agreement with Vegard's law [22].

3.2. Spin–lattice relaxation time T_1 measurements

The spin–lattice relaxation curves of $Rb_{0.23}(NH_4)_{0.77}I$ and $Rb_{0.71}(NH_4)_{0.29}I$ measured at frequency 59 MHz on cooling and heating of the samples at ambient pressure are shown in figure 2. For $Rb_{0.71}(NH_4)_{0.29}I$ in the whole studied temperature range 95–295 K on both cooling and heating, as well as for $Rb_{0.23}(NH_4)_{0.77}I$ on cooling from 295 to 125 K, the magnetization recovery was monoexponential with a relaxation time of the order of tens of seconds. The T_1 curve shows a flat maximum of ∼30 s at $T \sim 200$ K in both compounds. The shape of the T_1 curve is similar to one observed for the α and β phases of NH_4I in [23] at ambient pressure.

In $Rb_{0.23}(NH_4)_{0.77}I$, with the further temperature decrease below 120 K the magnetization recovery became biexponential. Apart from the component with a long relaxation time T_1 a component with a short relaxation time T_1 (the order of milliseconds) appeared, whose contribution increased with cooling the sample to lower temperatures. On heating, the magnetization recovery was biexponential up to 250 K, and the contribution of the short

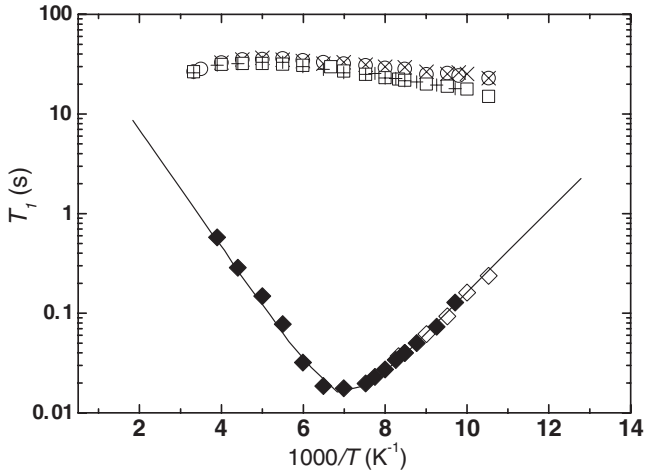

Figure 2. The temperature dependence of the spin–lattice relaxation time measured at resonance frequency 59 MHz and ambient pressure for $Rb_{1-x}(NH_4)_xI$, $x = 0.77$ (□, ◇—cooling, +, ♦—heating) and $x = 0.29$ (○—cooling, ×—heating).

relaxation time component decreased with heating the sample to higher temperatures. Above 250 K, the recovery of magnetization became monoexponential with a long relaxation time T_1. A similar behaviour of the magnetization with a large temperature hysteresis was observed at the phase transition to the tetragonal γ phase in the NMR study of NH_4I [23]. The component with a short relaxation time T_1 appears at a temperature close to one corresponding to the observation of the γ phase of $Rb_{0.23}(NH_4)_{0.77}I$ in neutron diffraction experiments, $T = 150$ K.

The magnetization component characterized by a short relaxation time T_1 in $Rb_{0.23}(NH_4)_{0.77}I$ reaches a minimum of 17.7 ms at 143 K. The minimum is broad and asymmetric (see figure 2). The slope of $\ln(T_1)$ versus $1000/T$ is lower on the low-temperature side of the minimum. The shortening of the relaxation time with increasing temperature on the high-temperature side of the T_1 maximum is caused by a spin-rotation interaction. For this interaction the rate of relaxation is inversely proportional to the correlation time [24]. The shortening of the relaxation time with decreasing temperature on the low-temperature side of the T_1 maximum is a result of dipolar interactions. For fast reorientations ($\omega_0\tau \ll 1$) the relaxation rate is directly proportional to the correlation time.

The behaviour of the magnetization component with a short relaxation time T_1 in $Rb_{0.23}(NH_4)_{0.77}I$ was interpreted by assuming the model of complex reorientations of the ammonium cation proposed in [25]. It takes into account the simultaneous reorientations of the ammonium ion around the two-fold and three-fold axes C_2 and C_3. The rate of relaxation is described by the formula

$$1/T_1 = (1/6)\gamma_p^2\Delta M_2[\tau_3/(1+\omega_0^2\tau_3^2) + 4\tau_3/(1+4\omega_0^2\tau_3^2) + 3\tau/(1+\omega_0^2\tau^2) + 12\tau/(1+4\omega_0^2\tau^2)], \quad (1)$$

where γ_p is the gyromagnetic ratio of the proton, ω_0 the angular resonance frequency, ΔM_2 the change of the second moment of the ^{1}H NMR line and $\tau = 1.5/(1/\tau_2 + 1/\tau_3)$. The correlation times τ_2 and τ_3 describe the reorientations about the axes C_2 and C_3, respectively, and are related to the enthalpies of activation ΔH_2^* and ΔH_3^* through the Arrhenius equation. The activation parameters for the reorientations about the C_2 and C_3 axes cannot be much different because only one albeit wide T_1 minimum is observed. The activation parameters (ΔH_2^*, ΔH_3^*,

Table 2. Activation parameters of $Rb_{1-x}(NH_4)_xI$ ($x = 0.77$, 0.29 and 1).

P (MPa)	ΔM_2 (G^2)	τ_c (10^{-13} s)	ΔH_2^* (kJ mol^{-1})	ΔH_3^* (kJ mol^{-1})
0.1 (59 MHz)				
$Rb_{0.23}(NH_4)_{0.77}I$		2.08	9.61	12.84
50				
$Rb_{0.71}(NH_4)_{0.29}I$	9.43	4.94	8.33	11.13
$Rb_{0.23}(NH_4)_{0.77}I$	10.02	2.13	9.83	12.13
NH_4I [23]	11.44	0.42	17.03	13.5
400				
$Rb_{0.71}(NH_4)_{0.29}I$	10.89	3.32	8.87	11.97
$Rb_{0.23}(NH_4)_{0.77}I$	10.01	1.59	9.58	12.59
NH_4I [23]	11.48	0.4	16.36	13.51
800				
$Rb_{0.71}(NH_4)_{0.29}I$	9.85	4.88	8.58	12
$Rb_{0.23}(NH_4)_{0.77}I$	9.05	6.23	8.74	10.84
NH_4I [23]	10.31	0.45	16.65	14.02

τ_2, τ_3 and ΔM_2) obtained from the best fit of the model of the ammonium ion reorientations (equation (1)) to the measured values are collected in table 2. The calculated values of ΔH_2^* and ΔH_3^* for $Rb_{0.23}(NH_4)_{0.77}I$ are smaller in comparison with the pure NH_4I [23]. The substitution of NH_4^+ by Rb^+ ions leads to an increase of the unit cell volume and interatomic distances, and as a consequence to the decrease of potential barriers for the ammonium reorientations corresponding to activation enthalpies ΔH_2^* and ΔH_3^*. In $Rb_{0.23}(NH_4)_{0.77}I$ the activation enthalpy for the reorientation about the C_2 axis is lower than that for the reorientation about the C_3 axis ($\Delta H_2^* < \Delta H_3^*$). For the pure NH_4I the opposite situation was found, ($\Delta H_2^* > \Delta H_3^*$) [23]. This observation may be attributed to local inhomogeneities of the interatomic potential in the mixed crystal $Rb_{0.23}(NH_4)_{0.77}I$ due to the presence of the statistical disorder of NH_4^+ and Rb^+ ions in the lattice.

In order to construct the P–T phase diagram for $Rb_{0.23}(NH_4)_{0.77}I$ and $Rb_{0.71}(NH_4)_{0.29}I$ crystals, the spin–lattice relaxation time T_1 measurements were performed at the resonance frequency 25 MHz in the pressure range 50–800 MPa and temperature range 95–300 K. For $Rb_{0.23}(NH_4)_{0.77}I$ at $T = 286$ K the relaxation time T_1 is constant and equal to about 26 s in the pressure range 50–150 MPa. At $P \approx 150$ MPa the relaxation time decreases jumpwise by an order of magnitude and then with increasing pressure it slowly decreases (see figure 3). Such behaviour is characteristic for the pressure-induced α–β phase transition [23]. At $T = 167$ K the relaxation time T_1 increases with increasing pressure up to 350 MPa. With a further pressure increase T_1 starts to decrease slightly (see figure 3). Similar features were observed in the NMR study of the P–T phase diagram of NH_4I [23], and the fracture of the T_1 pressure dependence is related to the β–γ phase transition. At 83 K T_1 decreases slightly in the pressure range from 50 to 650 MPa and it starts to increase at pressures above 650 MPa (see figure 3) with a slope higher than observed at 167 K in the pressure range 150–350 MPa. According to [23], the relaxation time T_1 shows a behaviour characteristic for the γ phase in the pressure range 0–650 MPa and the point of the change of the slope of the $T_1(P)$ curve corresponds to the γ–δ phase transition. A similar pressure dependence $T_1(P)$ is observed at 100 K, but the T_1 time starts to increase from 700 MPa. The $T_1(P)$ dependences measured on the pressure decrease are similar to those obtained with increasing pressure.

For $Rb_{0.71}(NH_4)_{0.29}I$ the T_1 pressure dependence measured at $T = 295$ K (see figure 4) is similar to that for $Rb_{0.23}(NH_4)_{0.77}I$. With a pressure increase, a jumpwise change in T_1 at

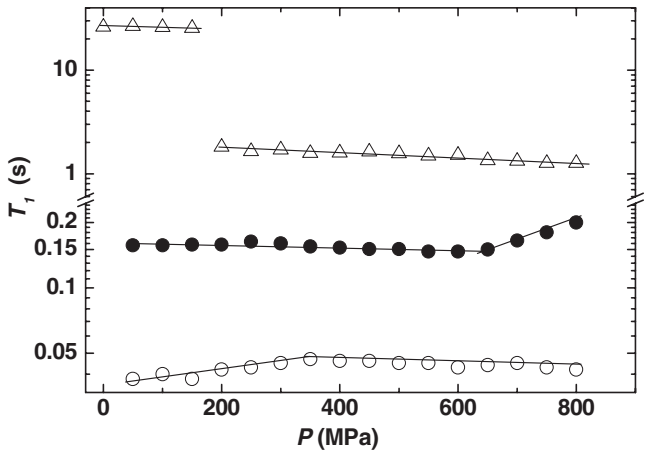

Figure 3. Pressure dependences of the spin–lattice relaxation time measured for $Rb_{0.23}(NH_4)_{0.77}I$ at 286 K (△), 167 K (○) and 87 K (●).

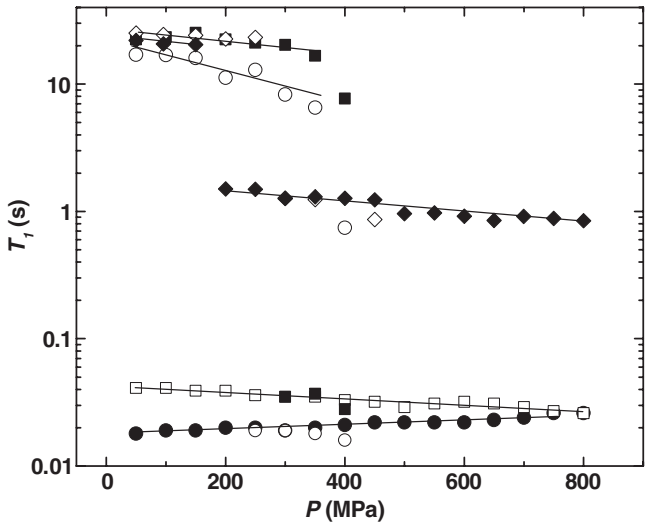

Figure 4. Pressure dependences of the spin–lattice relaxation time measured for $Rb_{0.71}(NH_4)_{0.29}I$ at 295 K (◇—on increasing pressure, ◆—on decreasing pressure), 167 K (■—on increasing pressure, □—on decreasing pressure) and 100 K (○—on increasing pressure, ●—on decreasing pressure).

$P = 300$ MPa takes place, indicating the α–β phase transition. The measurements performed on decreasing pressure revealed a jumpwise change in T_1 at 200 MPa. The pressure hysteresis was observed in the whole temperature range studied. At 167 K the relaxation time T_1 remains nearly constant in the pressure range 50–250 MPa and its value is about 22 s, similar to that for $T = 295$ K in the pressure range 50–300 MPa. Starting from $P = 300$ MPa the recovery of magnetization becomes biexponential and has a long- and a short-relaxation time component (see figure 4). With increasing pressure the contribution of the long time component decreases and that of the short time component increases. Above 400 MPa the magnetization recovery is monoexponential and is characterized by a short T_1 time. On further increasing the

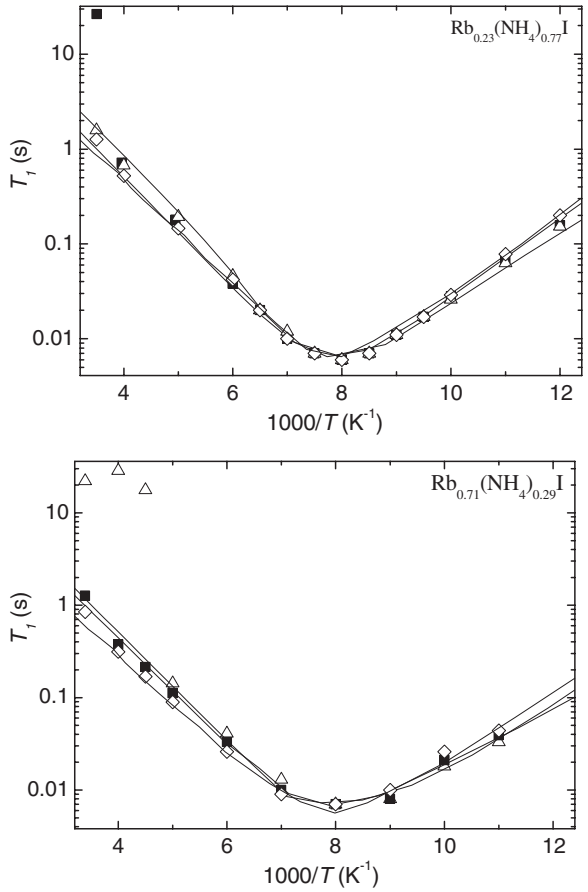

Figure 5. The temperature dependence of the spin–lattice relaxation time measured at different pressures for $Rb_{0.23}(NH_4)_{0.77}I$ (top), and $Rb_{0.71}(NH_4)_{0.29}I$ (bottom), ■—50 MPa, △—400 MPa, ◇—800 MPa.

pressure, T_1 decreases slightly. On decreasing the pressure the recovery of magnetization is monoexponential in the whole pressure range studied, and it is characterized by a short, slowly increasing T_1 time. At 100 K (see figure 4) the situation is very similar to that for 167 K. From a comparison with the $T_1(P)$ curves measured for $Rb_{0.71}(NH_4)_{0.29}I$ at 295 K one may conclude that the features observed in the pressure dependences of the T_1 relaxation time at $T = 167$ and 100 K correspond to the α–β phase transition.

The spin–lattice relaxation time T_1 curves as functions of inverse temperature measured at pressures 50, 400 and 800 MPa in $Rb_{0.23}(NH_4)_{0.77}I$ and $Rb_{0.71}(NH_4)_{0.29}I$ are shown in figure 5. At 50 MPa for $T > 250$ K in $Rb_{0.23}(NH_4)_{0.77}I$ and $T > 200$ K in $Rb_{0.71}(NH_4)_{0.29}I$ there is one long component of the relaxation time T_1, corresponding to the α phase. Below these temperatures only one short T_1 component was observed (in $Rb_{0.71}(NH_4)_{0.29}I$ on pressure decrease only). At pressures 400 and 800 MPa also just a short T_1 relaxation time component, characteristic of the β and γ phases of $Rb_{0.23}(NH_4)_{0.77}I$ and the β phase of $Rb_{0.71}(NH_4)_{0.29}I$, was found. The short T_1 component curve reaches a minimum at $T \approx 125$ K for all pressures studied; its value is about 6 ms for $Rb_{0.23}(NH_4)_{0.77}I$ and 7 ms for $Rb_{0.71}(NH_4)_{0.29}I$. In $Rb_{0.71}(NH_4)_{0.29}I$ at 50 MPa the T_1 minimum is observed on decreasing pressure only, due to the large pressure hysteresis of the α–β phase transition.

Table 3. The activation volume of $Rb_{1-x}(NH_4)_xI$ ($x = 0.77$, 0.29 and 1).

T (K)	Pressure range (MPa)	ΔV^* ($cm^3\ mol^{-1}$)	Phase
	$Rb_{0.23}(NH_4)_{0.77}I$		
286	200–800	1.17	β
167	50–350	0.98	β
167	350–800	0.15	γ
83	50–650	0.08	γ
83	650–800	1.32	δ
	$Rb_{0.71}(NH_4)_{0.29}I$		
295	300–800	2	β
167	800–50	0.84	β
100	800–50	0.41	β
	NH_4I [23]		
300	10–800	1.34	β
167	0–450	0	γ
167	500–800	3.09	δ
105	0–500	0	γ
105	550–800	1.45	δ

The activation parameters determined on the basis of the best fit of the high-pressure experimental data by equation (1) are collected in table 2. The parameters determined for $Rb_{0.23}(NH_4)_{0.77}I$ at 50 MPa and the resonance frequency 25 MHz are very similar to those determined at ambient pressure and the resonance frequency 59 MHz. For all pressures the activation enthalpy for the reorientation about the axis C_2 is smaller than that for the reorientation about the C_3 axis ($\Delta H_2^* < \Delta H_3^*$). The pressure variation of ΔH_2^* and ΔH_3^* does not exceed the error limits of their determination (about 10%) and they can be considered as constants in the pressure range studied, $\Delta H_2^* \approx 9.44\ kJ\ mol^{-1}$ and $\Delta H_3^* \approx 12.1\ kJ\ mol^{-1}$ for $Rb_{0.23}(NH_4)_{0.77}I$ and $\Delta H_2^* \approx 8.59\ kJ\ mol^{-1}$ and $\Delta H_3^* \approx 11.7\ kJ\ mol^{-1}$ for $Rb_{0.71}(NH_4)_{0.29}I$.

The experimental $T_1(P)$ data allow us to calculate the activation volume ΔV^* [26] for the different phases of $Rb_{0.23}(NH_4)_{0.77}I$ and $Rb_{0.71}(NH_4)_{0.29}I$, usually defined as a difference between the critical volume (needed for reorientation of a molecule or an ion) and the molar volume and expressed as

$$\Delta V^* = RT[\partial(\log_e T_1)/\partial P]_T. \tag{2}$$

This formula holds only for the relaxation times T_1 far from the minimum and where $\omega_0\tau \gg 1$ or $\omega_0\tau \ll 1$.

As was shown in [23], the activation volumes for the β, γ and δ phases of NH_4I are different and have characteristic values $(\Delta V^*)_\beta \sim 1.3$, $(\Delta V^*)_\gamma \sim 0$ and $(\Delta V^*)_\delta \sim 2.3\ cm^3\ mol^{-1}$. The calculated activation volumes of the β, γ and δ phases of $Rb_{0.23}(NH_4)_{0.77}I$ and the β phase of $Rb_{0.71}(NH_4)_{0.29}I$ are comparable with the corresponding values for NH_4I (see table 3). The value of $(\Delta V^*)_\gamma$ in $Rb_{0.23}(NH_4)_{0.77}I$ was found to be close to 0, as in NH_4I.

The P–T phase diagrams of $Rb_{0.23}(NH_4)_{0.77}I$ and $Rb_{0.71}(NH_4)_{0.29}I$ constructed on the basis of the experimental data obtained are shown in figure 6. The phase diagram of $Rb_{0.23}(NH_4)_{0.77}I$ resembles that of NH_4I [23] with four phases—α, β, γ and δ. The substitution of ammonium by 23% of rubidium shifts the α and β phase regions down to lower temperatures and the δ phase region up to higher pressures in comparison with NH_4I. The phase diagram of $Rb_{0.23}(NH_4)_{0.77}I$ is rather schematic, with few experimental points. Further detailed

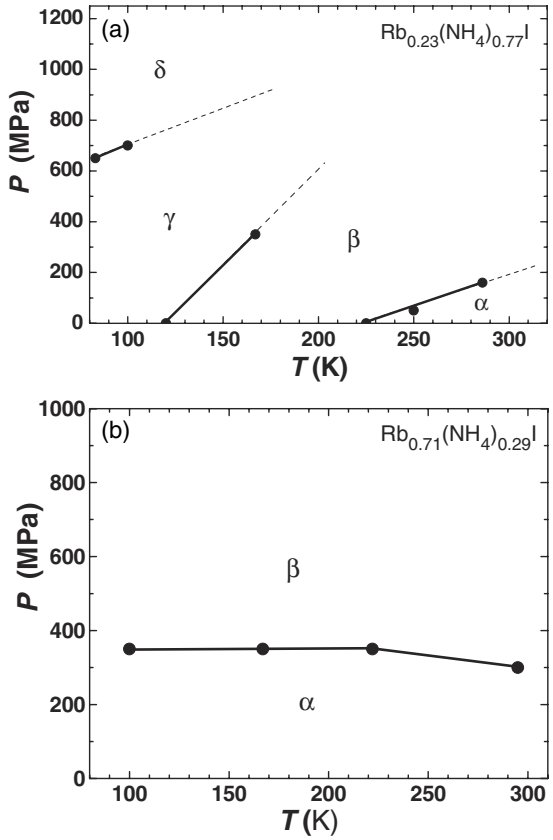

Figure 6. The proposed phase diagrams of (a) $Rb_{0.23}(NH_4)_{0.77}I$ and (b) $Rb_{0.71}(NH_4)_{0.29}I$. Only the experimental points obtained on pressure increase and temperature decrease are shown.

neutron diffraction investigations with deuterated samples would be helpful to confirm and improve it.

The phase diagram of $Rb_{0.71}(NH_4)_{0.29}I$ has only α and β phases in the studied temperature and pressure range, with a rather large hysteresis at the phase boundary. It resembles the phase diagram of RbI, which exhibits a phase transition from the NaCl-type cubic phase to the CsCl-type cubic phase at $P \sim 350$ MPa [27], also with a pressure hysteresis. In [17] it was concluded that $Rb_{0.71}(NH_4)_{0.29}I$ exhibits the orientational glass state at $T \sim 20$ K. For the temperature interval of the present study, 95–300 K, no indications of the orientational glass state formation in $Rb_{0.71}(NH_4)_{0.29}I$ were observed.

Within the four phases observed in the $Rb_{1-x}(NH_4)_xI$ mixed crystals studied, the α and β phases are common for both mixed crystals and parent compounds NH_4I and RbI. The α–β transition pressure P_t in $Rb_{1-x}(NH_4)_xI$ compounds increases linearly with the Rb content increase and related increase of the lattice parameter at ambient pressure (see figure 7), from 100 MPa (NH_4I [23]) to 350 MPa (RbI [27]).

4. Conclusions

In the present work the P–T phase diagram of $Rb_{1-x}(NH_4)_xI$ mixed crystals ($x = 0.29, 0.77$) has been investigated jointly by neutron powder diffraction and proton NMR techniques. Both

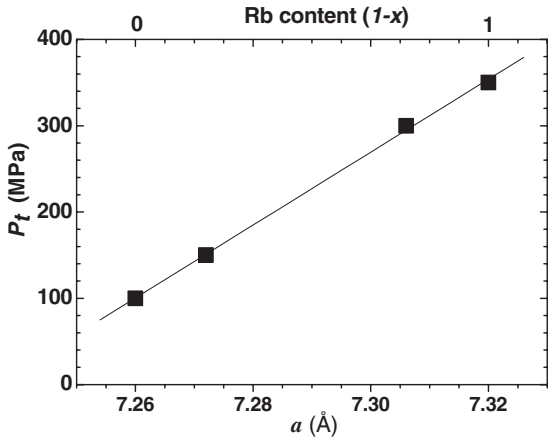

Figure 7. The α–β transition pressure P_t in $Rb_{1-x}(NH_4)_xI$ compounds as a function of the lattice parameter at ambient pressure and Rb content $(1 - x)$.

structural data obtained from neutron diffraction measurements at ambient pressure and specific features of the high-pressure behaviour of the spin–lattice relaxation time T_1 in the vicinity of phase transitions known from our previous study of NH_4I were used for the construction of the phase diagrams.

The phase diagram obtained of the ammonium-rich sample $Rb_{0.23}(NH_4)_{0.77}I$ is similar to that of NH_4I and contains α, β, γ and δ phases, with regions of the α and β phases shifted to lower temperatures and the δ phase region shifted to higher pressures. The phase diagram obtained of the rubidium-rich sample $Rb_{0.71}(NH_4)_{0.29}I$ contains only α and β phases with a noticeable hysteresis at the phase boundary, similar to that of RbI. The α–β transition pressure in $Rb_{1-x}(NH_4)_xI$ crystals increases linearly with the increase of Rb content.

The model of the complex ammonium ion reorientations about two-fold C_2 and three-fold C_3 axes can be successfully used to describe the experimental spin–lattice relaxation time data for the β, γ and δ phases of $Rb_{0.23}(NH_4)_{0.77}I$ and the β phase of $Rb_{0.71}(NH_4)_{0.29}I$. The activation enthalpy obtained for the reorientation about the C_2 axis is smaller than that for the reorientation about the C_3 axis, $\Delta H_2^* < \Delta H_3^*$ in the whole pressure range studied.

References

[1] Parsonage N G and Stavely L A K 1978 *Disorder in Crystals* (Oxford: Oxford University Press)
[2] Kozlenko D P, Belushkin A V, Knorr K, McGreevy R L, Savenko B N and Zetterström P 2001 *Physica* B **299** 46
[3] Fehst I, Böhmer R, Ott W, Loidl A, Haussühl S and Bostoen C 1990 *Phys. Rev. Lett.* **64** 3139
[4] Havighurst R J, Mack E Jr and Blake F C 1925 *J. Am. Chem. Soc.* **47** 29
[5] Bostoen C, Coddens G and Wegener W 1989 *J. Chem. Phys.* **91** 6337
[6] Paasch M, McIntyre G J, Reehuis M, Sonntag R and Loidl A 1996 *Z. Phys.* B **99** 339
[7] Güthoff F, Ohl M, Reehuis M and Loidl A 1999 *Physica* B **266** 310
[8] Paasch M, Winterlich M, Böhmer R, Sonntag R, McIntyre G J and Loidl A 1996 *Z. Phys.* B **99** 333
[9] Böhmer R, Fujara F and Hinze G 1993 *Solid State Commun.* **86** 183
[10] Winterlich M, Titze A, Hinze G and Böhmer R 1998 *Phys. Rev.* B **57** 14158
[11] Hinze G, Böhmer R, Zalar B and Blinc R 1997 *J. Phys.: Condens. Matter* **9** 117
[12] Blinc R, Apih T, Dolinšek J, Šprogar M and Zalar B 1995 *Phys. Rev.* B **52** 15217
[13] Berret J-F, Sauvajol J-L and Haussühl S 1992 *J. Chem. Phys.* **96** 4896
[14] Berret J-F and Sauvajol J-L 1994 *Phys. Rev.* B **49** 15588

[15] Knorr K, Krimmel A, Loidl A and Depmeier W 1997 *Physica* B **234–236** 407
[16] Knorr K and Krimmel A 1998 *Solid State Commun.* **105** 419
[17] Smirnov L S, Natkaniec I, Savenko B N, Kozlenko D P, Kichanov S E, Dlouha M, Vratislav S, Martinez-Sarrion M L, Mestres L, Heraiz M and Shuvalov L A 2004 *Crystallogr. Rep.* **49** 1
[18] Aksenov V L, Balagurov A M, Glazkov V P, Kozlenko D P, Naumov I V, Savenko B N, Sheptyakov D V, Somenkov V A, Bulkin A P, Kudryashev V A and Trounov V A 1999 *Physica* B **265** 258
[19] Lewicki S, Pajak Z, Porzuckowiak W and Wasicki J 1995 *Proc. 28th NMR Seminar Report 1717/PL (Krakow)* p 190
[20] Zlokazov V B and Chernyshev V V 1992 *J. Appl. Crystallogr.* **25** 447
[21] Levy H A and Peterson S W 1952 *Phys. Rev.* **86** 766
[22] Vegard L 1921 *Z. Phys.* **5** 17
[23] Kozlenko D P, Lewicki S, Wąsicki J, Kozak A, Nawrocik W and Savenko B N 2001 *Mol. Phys.* **99** 427
[24] Farrar T C and Becker E D 1971 *Pulse and Fourier Transform NMR Introduction to Theory and Methods* (New York: Academic)
[25] Watton A 1976 *J. Chem. Phys.* **65** 3653
[26] Anderson J W and Slichter W P 1966 *J. Chem. Phys.* **44** 1797
[27] Blaschko O, Ernst G, Quittner G, Pépy G and Roth M 1979 *Phys. Rev.* B **20** 1157